Geophysical Research Letters

RESEARCH LETTER
10.1029/2024GL114073

Upper Mantle Earthquakes Along the Edge of the Wyoming Craton

Sean J. Hutchings[1], Keith D. Koper[1], Relu Burlacu[1], Qicheng Zeng[1], Fan-Chi Lin[1], and George Zandt[2]

[1]Department of Geology and Geophysics, University of Utah, Salt Lake City, UT, USA, [2]Department of Geosciences, University of Arizona, Tucson, AZ, USA

Key Points:

- We document the occurrence of nine small earthquakes in the upper mantle beneath Wyoming and Utah between 1979 and 2023
- The earthquakes occurred along the western edge of the Wyoming Craton at relatively high temperatures (>700°C)
- Brittle and ductile (thermal runaway) source processes are likely facilitated by relatively high strain rates from mantle convection

Supporting Information:

Supporting Information may be found in the online version of this article.

Correspondence to:

S. J. Hutchings,
sean.hutchings@utah.edu

Citation:

Hutchings, S. J., Koper, K. D., Burlacu, R., Zeng, Q., Lin, F.-C., & Zandt, G. (2025). Upper mantle earthquakes along the edge of the Wyoming Craton. *Geophysical Research Letters*, *52*, e2024GL114073. https://doi.org/10.1029/2024GL114073

Received 10 DEC 2024
Accepted 20 MAR 2025

Abstract Earthquakes in continental regions overwhelmingly occur in the crust where low pressure and temperature promote brittle failure in response to tectonic stress. In rare cases, primarily in the thickened lithosphere near the Himalayas and Tibet, continental earthquakes occur in the uppermost mantle, perhaps implying an abnormally deep brittle-ductile transition zone created by relatively low temperatures ($\lesssim$600°C) and the increased strength of olivine-rich mantle rocks. Here we present evidence for nine mantle earthquakes—only four of which were previously recognized—along the edge of the Wyoming Craton in the western U.S. Eight of the nine earthquakes occurred >15 km beneath the Moho where temperatures are likely above 700°C. We infer a mixture of brittle and ductile (thermal runaway) source processes facilitated by elevated strain rates from regional or edge-driven mantle convection, which is thought to be a primary force behind crustal seismicity in the Intermountain West.

Plain Language Summary Continental earthquakes typically occur in the uppermost 10 km of the crust. In rare cases, they can occur deeper in the uppermost mantle. The Intermountain West of the U.S. provides convincing evidence of intraplate upper mantle seismicity on the edge of the ancient Wyoming Craton in Utah and Wyoming, a portion of the stable interior of the North American continent. We present the most up to date map of upper mantle seismicity—nine confirmed events in total—beneath the Wyoming Craton through verification of earthquake depths and comparisons to crustal thickness. We find that these earthquakes are likely occurring in ductile mantle material at temperatures exceeding 700°C and are located in areas exhibiting rapid changes in lithospheric thickness. These earthquakes are likely facilitated by regional or localized mantle convective forces interacting with complex lithospheric structure, which is suspected to be a leading cause of crustal seismicity in the Intermountain West.

1. Introduction

Earthquakes in the continental mantle are extremely rare and have primarily been observed beneath the thickened crust of the Himalayas and Tibet (e.g., Chen & Molnar, 1983; Molnar & Chen, 1983). Though debate about their existence arose due to difficulty in resolving earthquake depths with teleseismic arrival times and uncertainty about Moho depth (Maggi et al., 2000), several studies, using a variety of seismological techniques, have confirmed their existence in the uppermost mantle (e.g., Michailos et al., 2021; Monsalve et al., 2006; Schulte-Pelkum et al., 2019; Song & Klemperer, 2024; Wang & Klemperer, 2021; L. Zhu & Helmberger, 1991). These uncommon earthquakes provide insight into lithospheric structure, composition, temperature, and strength, allowing inferences on continental evolution and dynamics (Jackson et al., 2021).

Mantle lithologies are generally stronger than those of continental crust, and at temperatures ~600°C the uppermost mantle may undergo brittle deformation while the lower crust deforms ductiley, referred to as the "jelly sandwich" rheological model (e.g., Burgmann & Dresen, 2008). Alternatively, thickened and anhydrous continental lithosphere may allow for continuous seismicity throughout the crust and upper mantle if temperatures remain <600°C, referred to as the "caramel slab" model (Chen et al., 2013). In either case, upper mantle earthquakes beneath the Himalayas and Tibet have been used to infer the presence of a strong and cold lithospheric mantle (Chen & Yang, 2004), with similar inferences made for upper mantle earthquakes in northern Australia (Sloan & Jackson, 2012) and portions of the East African Rift system (Yang & Chen, 2010). However, other research has suggested that cold temperatures are not required for mantle earthquakes when strain rates are high (e.g., Molnar, 2020). In particular, if strain rates are sufficiently high, a plastic instability known as thermal

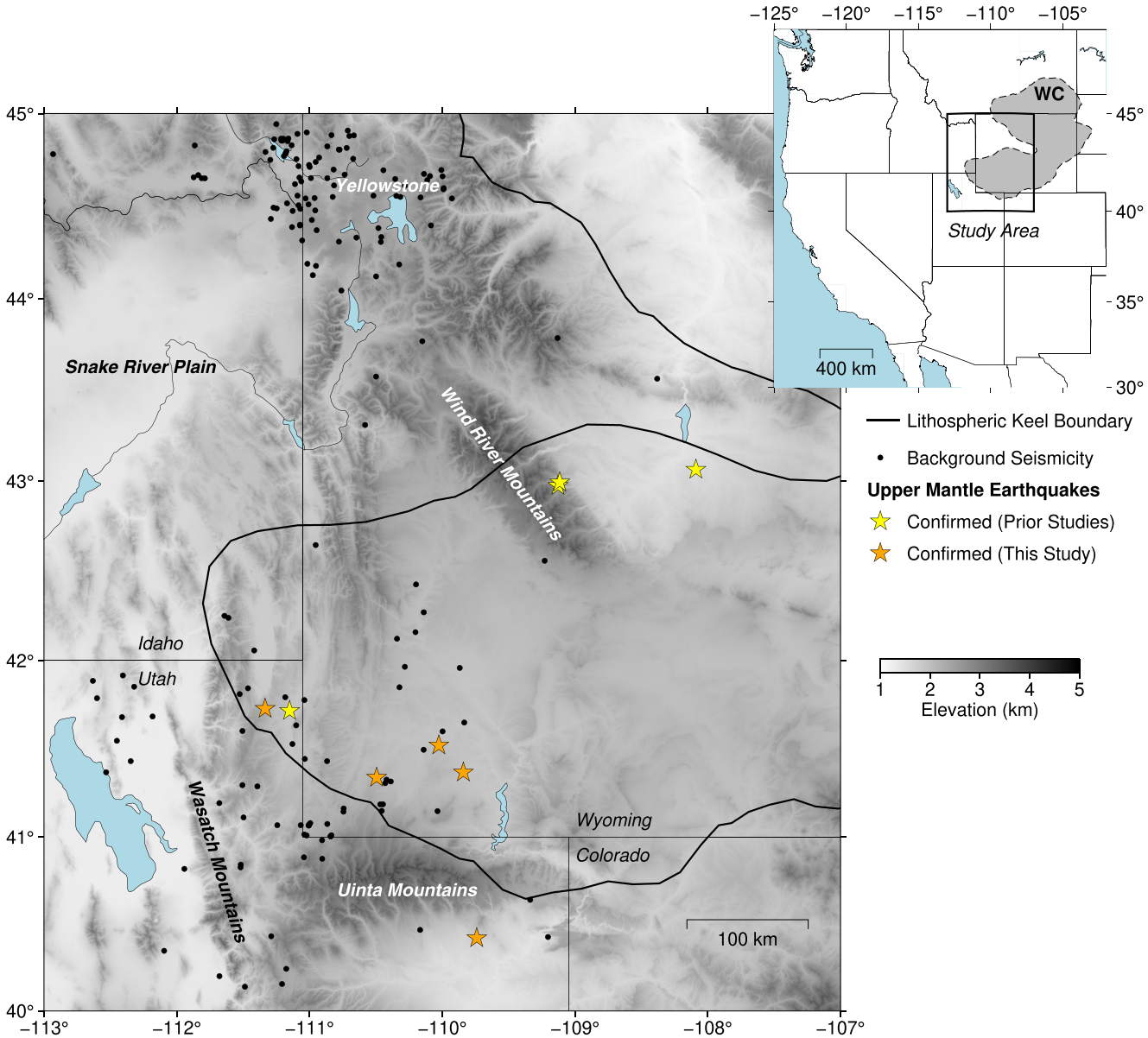

Figure 1. Map of the study region. Mantle earthquakes are shown as stars. Black dots show background seismicity (1979–2023) suspected to be in the mid-to-lower crust at depths >20 km. The thick black line represents a depth-averaged (60–125 km) high resistivity contour interpreted as the boundaries of the lithospheric keel of the Wyoming Craton (shaded gray region in the inset map labeled "WC") defined by Bezada et al. (2024).

runaway could generate continental mantle earthquakes with shear-faulting mechanisms similar to brittle failure (Thielmann, 2018).

The most compelling evidence for continental mantle seismicity outside of the Himalayas and Tibet lies in the Intermountain West of the United States, on the western margin of the Wyoming Craton (Figure 1). Located at the boundary of the tectonically active western U.S. and the stable interior of the North American plate, the western edge of the craton has been heavily eroded, creating heterogeneous structure and an overall thinning of the lithosphere westward across the states of Wyoming, Idaho, and Utah (e.g., Bezada et al., 2024; Dave & Li, 2016; Levander & Miller, 2012). An M_L 3.8 earthquake in northeastern Utah at a depth of 90 km was reported in 1979, and although its location accuracy has been questioned (Frohlich et al., 2015), an analysis supporting its mantle depth was presented in a meeting abstract (Zandt & Richins, 1979). More recently, an M_L 1.5 earthquake in 2010 was located at a depth of 63 km in central Wyoming using arrival time data from a temporary regional array of

Table 1
Relocation Summaries

Origin time (UTC)	Latitude (°N)	Longitude (°W)	Catalog depth (km)	Magnitude	Relocated depth (km)	Moho depth (km)	Focal temperature (°C)
24 February 1979 12:43:41	41.717	111.148	90.5	3.8 M_L	94.4 ± 1.8	37 ± 3	1,227.0 ± 46.9
29 March 1992 03:35:43	41.729	111.334	54.4	1.0 M_C	56.7 ± 1.8	37 ± 2	942.6 ± 62.1
18 June 2010 03:35:43	43.064	108.089	63.2	1.5 M_L	69.6 ± 3.0	46 ± 3	1,001.3 ± 68.4
21 September 2013 13:16:33	42.975	109.128	76.2	4.8 M_w	75.5 ± 2.3	44 ± 2	993.2 ± 66.4
21 September 2013 15:15:34	42.994	109.115	71.4	3.0 M_L	76.9 ± 2.2	44 ± 2	1,001.7 ± 65.9
23 December 2019 22:34:08	41.522	110.026	60.5	3.2 M_L	57.8 ± 1.5	40 ± 2	840.7 ± 67.9
21 April 2020 07:59:24	41.368	109.841	45.5	2.4 M_L	44.5 ± 1.2	40 ± 1	493.8 ± 70.0
15 December 2020 11:41:50	40.421	109.740	55.8	1.4 M_L	56.0 ± 2.0	43 ± 1	965.8 ± 57.7
23 August 2023 15:54:39	41.339	110.494	58.8	2.3 M_L	56.2 ± 2.2	39 ± 2	789.9 ± 67.4

Note. Origin time, latitude, longitude, and magnitude are catalog values. Relocated depth is the mean depth plus or minus one standard deviation. Moho depth is the median depth from all investigated models plus or minus one median absolute deviation (MAD) (Table S3 in Supporting Information S1). All depths are relative to sea level. Temperatures are estimated at the relocated focal depth (Figure S16 in Supporting Information S1). Error is the interpolated thermal model uncertainties (Schutt et al., 2018; Shinevar et al., 2023).

seismometers (O'Rourke et al., 2016). Most convincing are two earthquakes that occurred in 2013 beneath the Wind River Range of central Wyoming: an M_w 4.8 mainshock at 76 km depth and its lone M_L 3.0 aftershock at 72 km depth (USGS ComCat). The mainshock was recorded with high signal-to-noise ratio enabling the use of multiple regional and teleseismic depth estimation techniques (e.g., Craig & Heyburn, 2015).

Here we present the most complete map of upper mantle seismicity near the Wyoming Craton to date (Figure 1). Nine earthquakes—five of which are newly evaluated in this study—are confirmed as originating in the mantle via comparison to 14 recent regional models of crustal thickness. We find that these earthquakes are located near the western edge of the craton, and we discuss their implications for tectonics and seismogenesis.

2. Earthquake Relocation

We searched the earthquake catalog of the University of Utah Seismograph Stations (UUSS, Pankow et al., 2020), the Comprehensive Catalog of the U.S. Geological Survey (USGS Comcat), and the existing scientific literature to identify nine events with depths >40 km that are plausibly located in the upper mantle of the study region (Figure 1, Table 1). Regional distance waveform data are available digitally for eight of the evaluated earthquakes, with data for the 1979 M_L 3.8 Randolph earthquake residing on analog microfilm records (Figure S1 in Supporting Information S1). The analyst reviewed arrival times for this event are presented in Table S1 in Supporting Information S1.

We apply a straightforward relocation methodology to resolve and verify focal depths. For each earthquake with waveform data, we inspect published arrival times, adjust them as necessary, grade their quality, and, when applicable, add picks to increase azimuthal coverage. Station distributions are summarized in Table S2 in Supporting Information S1, and example phase picks are presented in Figures S1 and S2 in Supporting Information S1. We perform relocations with ELOCATE (Herrmann, 2013) and seven 1D velocity models (Figure S3 in Supporting Information S1) that are used by the UUSS, USGS, and other earthquake agencies, as well as HYPOINVERSE (Klein, 2002), which uses a mixture of 1D velocity models and a different linearized inversion method. For each event and model, arrival times are stochastically perturbed using a Gaussian distribution 100 times, yielding a total of 800 relocations which are merged into a single population to calculate a mean and standard deviation for focal depth. Higher quality picks (0–1 weight) are perturbed with a standard deviation of 0.1 s, and lower quality picks (2–4 weight) are perturbed with a standard deviation of 0.2 s (Figure S2 in Supporting Information S1). This methodology is designed to account for variations in crustal structure and arrival time picking.

An example of this procedure is presented for the 1979 M_L 3.8 Randolph earthquake in Figure 2, yielding a focal depth of 94.4 ± 1.8 km. The uncertainty represents one standard deviation, and depth is relative to sea level. The original UUSS catalog depth, which was derived with a different inversion technique and velocity model, is

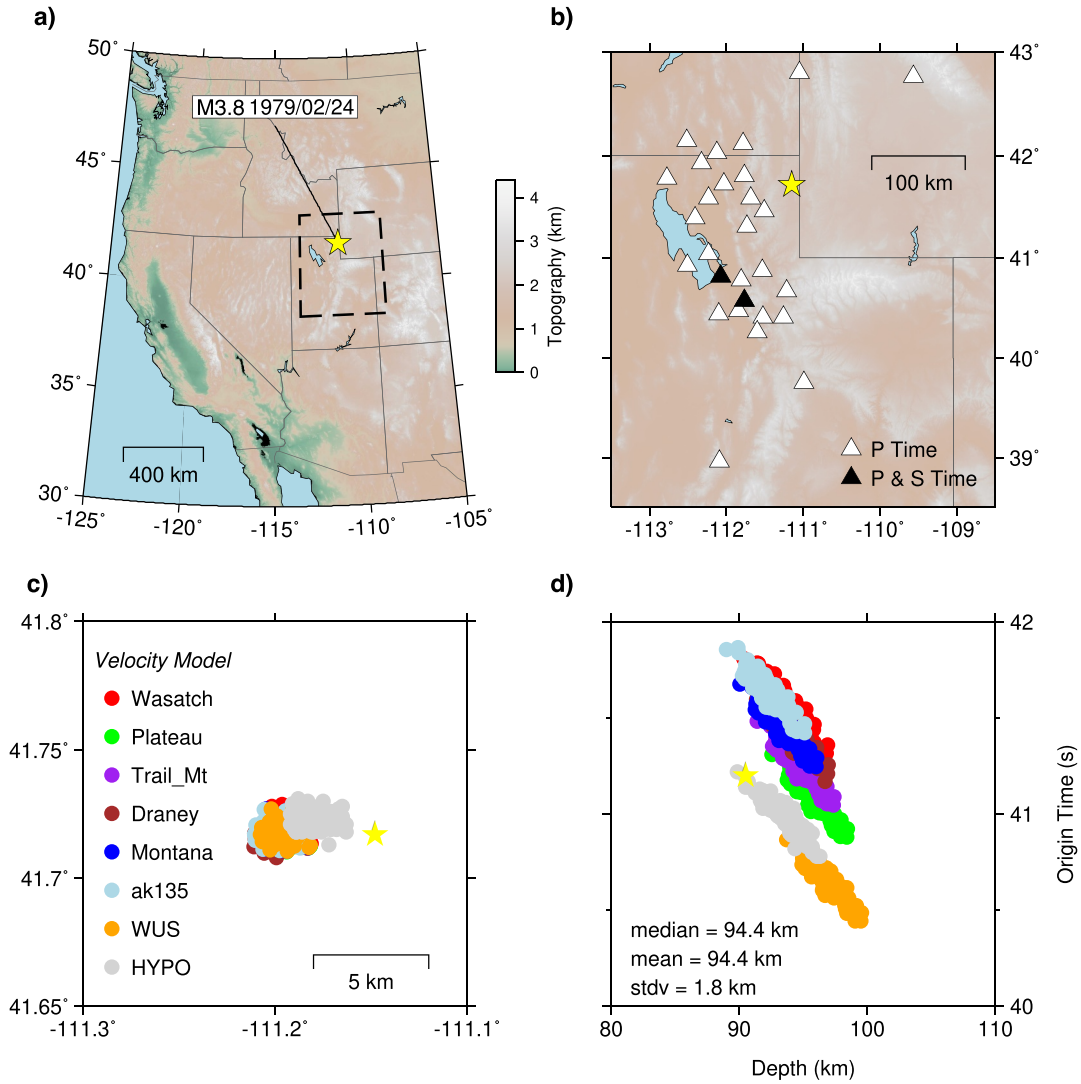

Figure 2. Relocation results for the 1979 M_L 3.8 earthquake near Randolph, Utah. (a) UUSS catalog epicenter (yellow star). Dashed box outlines the region shown in panel (b). (b) Station locations (triangles) with arrival times used. (c) Epicenters (circles) from stochastic perturbation of arrival times. Results for the Wasatch, Plateau, Trail_Mt., Draney, Montana, ak135, and WUS 1D velocity models are computed with the ELOCATE program (Herrmann, 2013), while HYPO are results from using the HYPOINVERSE program (Klein, 2002). (d) Depths and origin times for each model and method. Depth is relative to sea level and origin time is seconds after 12:43:00 UTC on 24 February 1979. Note that focal depth is relatively insensitive to the velocity model.

90.5 km. Our level of uncertainty is comparable to that of Pyle et al. (2023), who similarly evaluated the effects of variations in arrival times, velocity models, and inversion techniques on the locations of small crustal earthquakes recorded at local-to-regional distances in Nevada. The excellent depth resolution is owing to the existence of arrival times across a range of epicentral distances, with 8 picks from stations closer than 1.0 focal depth and 22 picks from stations at distances of 1.0–3.5 focal depths. Two S picks at distances of 126 and 137 km also improved depth resolution. Additional sensitivity tests are presented in Text S1 and Figures S4–S7 in Supporting Information S1. Our preferred depth remains 94–95 km but the standard deviation roughly doubles to 4–5 km in the case of deleted arrival times (Figure S6 in Supporting Information S1). Relocation results for the remaining eight earthquakes are shown in Figures S8–S15 in Supporting Information S1 and summarized in Table 1.

For all nine earthquakes, the original catalog depth is close to the range of relocated depths, which is usually on the order of a few kilometers. In most cases, our preferred depths are slightly greater than the catalog depths. Our results for the 2013 M_w 4.8 earthquake near Fort Washakie, WY, (Figure S8 in Supporting Information S1) validate our relocation methodology due to the consistency of our depth estimate with those from other

techniques and researchers. We find a depth of 75.5 ± 2.3 km using 22 P arrival times and 7 S arrival times recorded at distances of 44–243 km, while the USGS reported a depth of 76.2 km using 457 arrival times from phases including P, S, pP, sP, PcP, and PKP recorded at local-to-teleseismic distances. Previously estimated depths of ∼75 km, and 75 ± 8 km were obtained from an inversion of regional distance waveforms (Frohlich et al., 2015), and regional waveform inversion combined with teleseismic array-based analysis of depth phases (Craig & Heyburn, 2015), respectively. In general, we find that although focal depth trades off with origin time for a given velocity model, the range of acceptable depths is similar for different velocity models. Instead, origin time tends to trade off more strongly with velocity. This relationship manifests in the near-vertical alignment of depth-vs.-origin time clusters for different velocity models (Figure 2).

3. Moho Depths

Crustal and upper mantle properties in the Intermountain West of the U.S. are well resolved from decades of continuous monitoring by regional seismic networks (Pankow et al., 2020) and the Earthscope Transportable Array (TA) project (Long et al., 2014). While the TA was active (roughly 2006–2010 in the Intermountain West), high-quality, three-component broadband seismograph stations were uniformly deployed for 18–24 months with a nominal spacing of 75 km, allowing modern methods of seismic imaging to be applied by multiple independent research groups. We compiled Moho depth estimates in the region from 14 models presented in 13 publications (Table S3 in Supporting Information S1). These models were created via independent methodologies including active source seismology, P_n tomography, P and S receiver functions, Rayleigh wave dispersion and ellipticity, and gravity, with several researchers combining methods. Crustal thickness estimates are corrected to be relative to sea-level by subtracting the average elevation in the area. The model estimates for Moho depth that are closest to each epicenter are used, and the median and median absolute deviation (MAD) are calculated to compare to the relocated focal depths (Figure 3). Within two MAD, all nine earthquakes are located below the Moho. Eight are more than ∼15 km beneath the Moho, with the 2020 M_L 2.4 event about ∼5 km beneath the Moho. The most anomalous event is the 1979 M_L 3.8 earthquake which is ∼60 km beneath the Moho.

4. Mantle Temperatures

Upper mantle temperatures can be inferred from shear wave velocities, surface heat flow observations, and geochemical analysis of mantle xenoliths, providing insight into possible deformation mechanisms. Here we use two recent 3D temperature models of the western U.S. One study (Schutt et al., 2018) converted P_n velocity and crustal thickness (Buehler & Shearer, 2017) into Moho temperatures assuming a uniform spinel lherzolite composition and found a temperature range of ∼500°C–900°C in our study region (Figure 4). A second study (Shinevar et al., 2023) converted a recent mantle tomographic model (Golos et al., 2020) into estimates of temperature, composition, and density for a range of ultramafic lithologies and found temperatures of ∼700°C–1,250°C at depth slices of 60, 80, and 100 km in our study region (Figures 3b–3d). We acknowledge that significant uncertainties exist when converting seismic velocity into temperature (e.g., Lebedev et al., 2024), however the Shinevar et al. (2023) model was validated against temperatures inferred from young (<10 Ma) mantle xenoliths with good general agreement.

We construct mantle geotherms for each earthquake using nearest model points to the mean epicentral locations and linearly interpolating between the four temperature estimates provided by the two temperature models. We adopt the formal model uncertainties from these two studies, and our preferred temperatures are presented in Figure 3 and Table 1. Example geotherms are presented in Figure S16 in Supporting Information S1 along with previously estimated geotherms developed from steady state heat flow (Hasterok & Chapman, 2011; Wong & Chapman, 1990) and other velocity models (Prieto et al., 2017; Tesauro et al., 2014). Surface heat flow exceeds 55 mW/m^2 in the vicinity of the earthquakes (Blackwell et al., 2011; Lucazeau, 2019), which is higher than typical cratonic values (Hasterok & Chapman, 2011). Based on our interpolated temperature estimates, eight of the nine earthquakes appear to have nucleated at temperatures >700°C.

5. Focal Mechanisms

Several independent moment tensors derived for the largest event, the 2013 M_w 4.8 earthquake, show a double-couple with highly oblique strike-slip motion (USGS ComCat, Craig & Heyburn, 2015; Ekström et al., 2012; Frohlich et al., 2015; Herrmann et al., 2011). First motions for the eight smaller earthquakes exhibit variations in

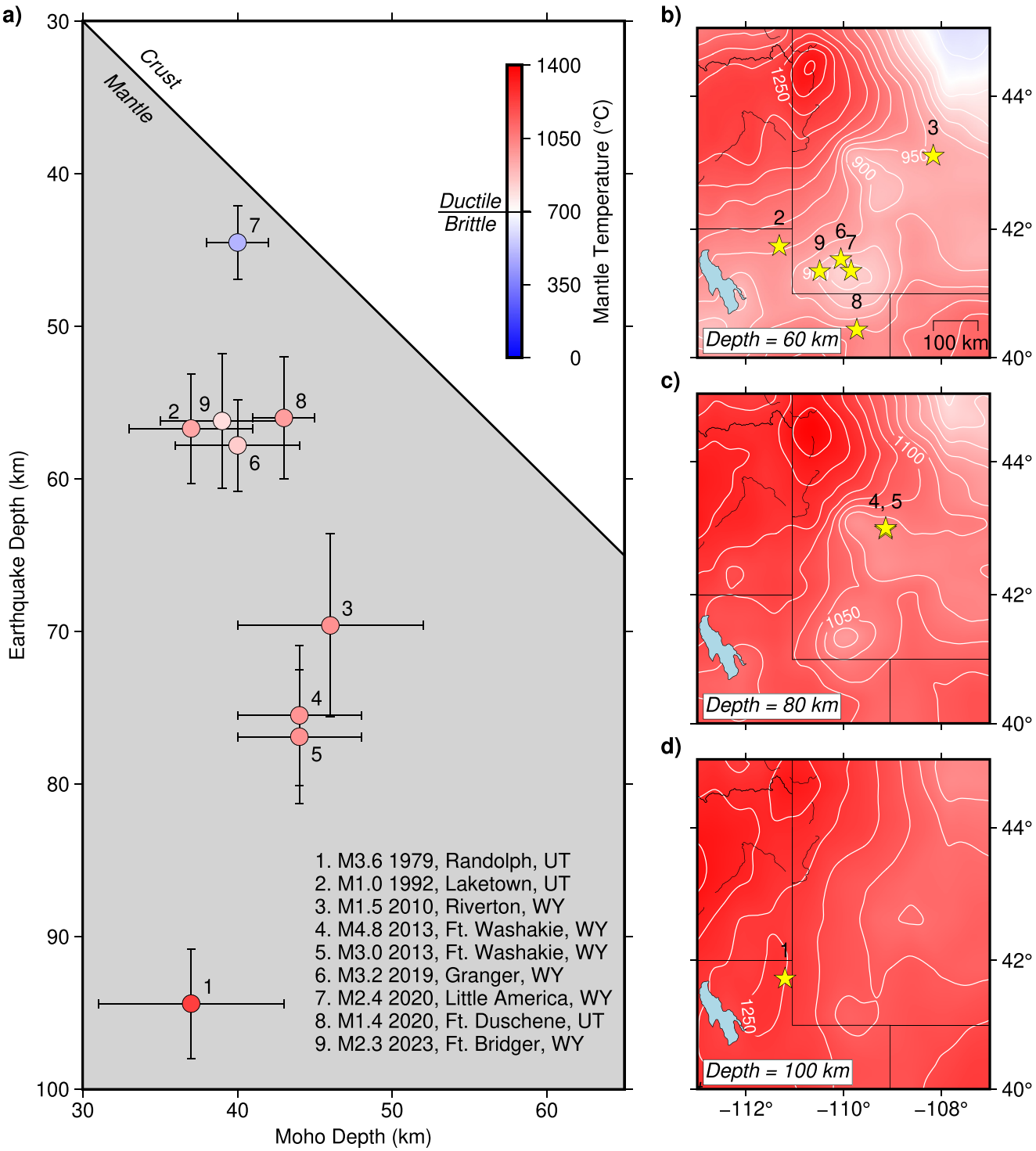

Figure 3. (a) Comparison of Moho depths and relocated focal depths. Moho depths are median estimates from the studies in Table S3 in Supporting Information S1. Horizontal error bars denote twice the median absolute deviation. Relocated earthquake depths are mean values. Vertical error bars denote two standard deviations. The brittle-ductile transition is conservatively estimated at ~700°C, assuming an anhydrous peridotitic mantle (Molnar, 2020) inferred from resistivity (e.g., Bedrosian & Frost, 2023). Temperature fields are shown at depths of (b) 60, (c) 80, and (d) 100 km (Shinevar et al., 2023). Ductile behavior is expected throughout most of the upper mantle, and earthquakes closest to each depth slice are plotted on the respective panel. C.I. = 50°C.

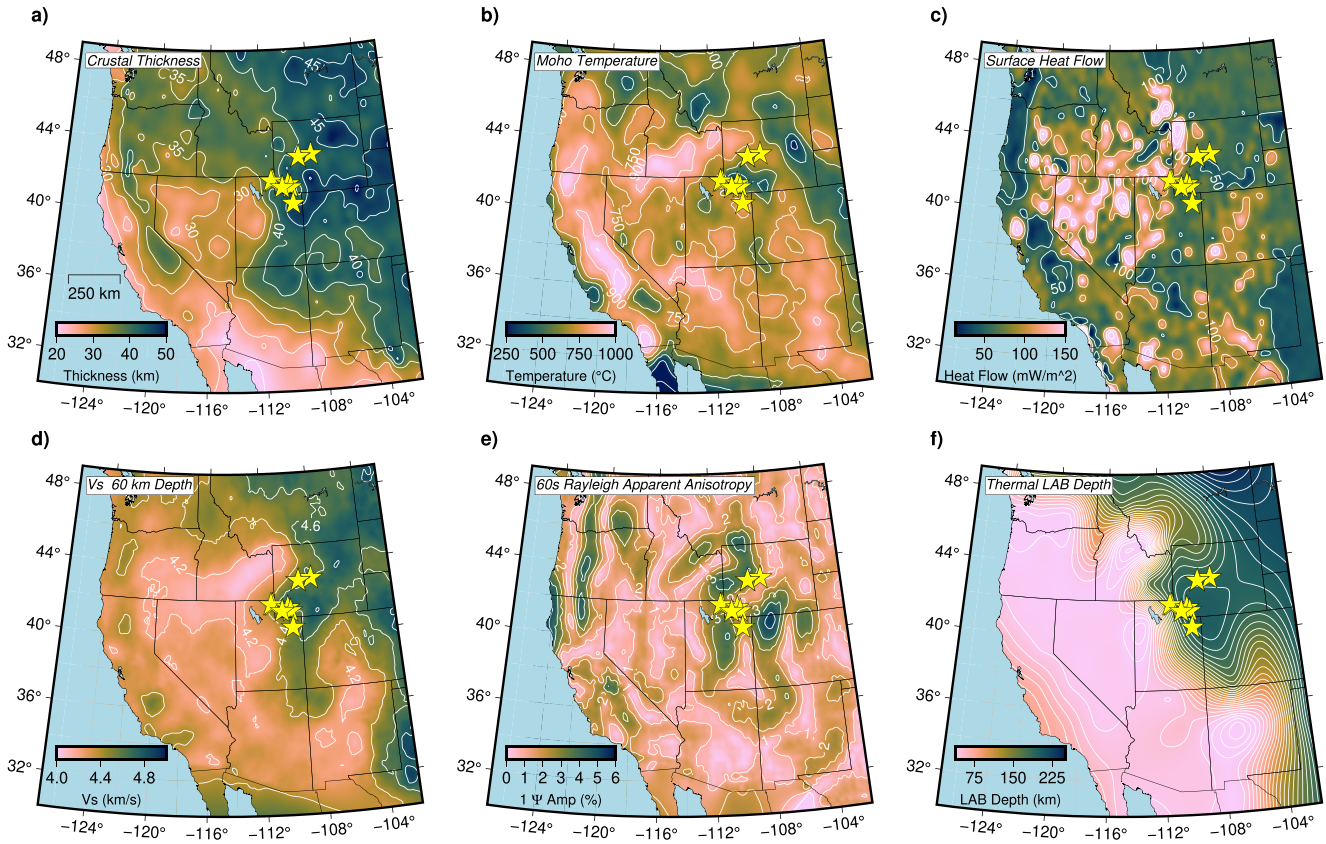

Figure 4. Earthquake epicenters (yellow stars) compared to (a) crustal thickness (Buehler & Shearer, 2017), (b) Moho temperature (Schutt et al., 2018), (c) surface heat flow (Lucazeau, 2019), (d) mantle shear velocity (Schmandt et al., 2015), (e) amplitude of the 1Ψ component of 60 s Rayleigh wave apparent anisotropy (Zeng et al., 2024), and (f) depth to the thermal lithosphere-asthenosphere boundary (Priestley et al., 2024). Lithospheric edges are emphasized in panels (d–f), though the long-wavelength model in panel (f) seems to underestimate the amount of erosion beneath the northwestern section of the Wyoming Craton that is observed in high resolution regional studies (e.g., Bezada et al., 2024; Dave & Li, 2016).

polarity consistent with double-couple mechanisms, thus there is no evidence for a dominantly isotropic mechanism that might indicate magma-assisted seismogenesis, such as dike emplacements proposed to explain upper mantle seismicity in magmatically active portions of the East African Rift (e.g., Lavayssière et al., 2019; Lindenfeld & Rümpker, 2011; Lindenfeld et al., 2012). We attempt to constrain focal mechanisms for these smaller events to gain insight into the stress field by inverting first motions with a search process that accounts for uncertainties in the velocity model and thus take-off angles (Skoumal et al., 2024). We achieve robust solutions for the 2013 M_w 4.8 (for method verification) and 2019 M_L 3.2 earthquakes (Figures S17 and S18 in Supporting Information S1). Both solutions exhibit oblique strike-slip motion with a T axis indicative of E-W oriented extension, broadly consistent with the regional stress field in the crust.

6. Discussion and Conclusions

6.1. Possible Mechanisms of Seismogenesis

Continental mantle earthquakes have sometimes been interpreted as brittle failure in localized heterogeneities embedded within a matrix of ductile material (Inbal et al., 2016). Here, we observe continental mantle earthquakes over a broad area (~30,000 km^2) at a variety of depths (5–60 km beneath the Moho) making brittle failure within isolated compositional heterogeneities less plausible. Our temperature estimates—and independent estimates for the 2013 M_w 4.8 and 1979 M_L 3.8 events (Prieto et al., 2017)—suggest a ductile process known as thermal runaway (Thielmann, 2018) is responsible for most of the mantle earthquakes near the Wyoming Craton analyzed in this study. This process localizes strain through a velocity weakening and grain size reduction feedback loop, and has been suggested as a possible mechanism for events with dissipative source processes (e.g.,

low rupture velocity and radiation efficiency; Zhan, 2020) as observed for the 2013 M_w 4.8 earthquake (Prieto et al., 2017). The aftershock deficiency observed for events studied here is also consistent with that of deep subduction zone earthquakes occurring in relatively warm environments (Wiens & McGuire, 1995).

However, thermal runaway is not needed for all the evaluated earthquakes, as temperatures near the M_L 2.5 2020 Little America earthquake suggest brittle deformation near the Moho. Therefore, it is likely that a combination of brittle and ductile mechanisms actively contribute to mantle deformation depending on depth and local conditions, which has been recognized in other regions where seismicity crosses the Moho (e.g., Schulte-Pelkum et al., 2019). While much of the lithosphere here is suspected to be compositionally anhydrous (Bedrosian & Frost, 2023), Zhao et al. (2024) proposed that the 2013 Wind River earthquakes were induced by ascending fluids sourced from dehydration reactions in the remnant Farallon slab, currently suspected to reside below the craton at a depth of ∼300 km. Considering this model and the variability in resistivity structure at the edges of the Wyoming Craton (Bedrosian & Frost, 2023; Bezada et al., 2024), the presence of fluids in the vicinity of the earthquakes cannot be ruled out and may provide additional incentive for rupture.

6.2. Link to Lithospheric Edges

Regardless of the source mechanism, a unifying factor that links the earthquakes explored here is their proximity to complex lithospheric structure (Figure 4). The epicenters are correlated with several geophysical quantities that are indicative of lithospheric edges: steep changes in the depth to the thermal lithosphere-asthenosphere boundary (LAB, Priestley et al., 2024), rapid lateral changes in mantle shear velocity (Schmandt et al., 2015), and large magnitude of the 1Ψ component of directionally dependent Rayleigh wave phase velocity at 60 s (Zeng et al., 2024). The latter quantity relates to structural heterogeneity in the upper mantle and can be simulated using velocity models with lateral step-like changes in velocity (Zeng et al., 2024). All nine earthquakes are located within 100 km of the recently imaged lithospheric keel of the Wyoming Craton by Bezada et al. (2024) (Figure 1), which suggests substantial heterogeneity in lithospheric structure and erosion of the craton at depths of 60–125 km.

Regional mantle convection—likely driven by thermal anomalies in the Basin and Range and upwelling associated with the Yellowstone plume—interacting with lithospheric edges has been proposed as a major driver of intraplate deformation in the Intermountain West (Becker et al., 2015; Cao & Liu, 2024; Castellanos et al., 2022). Localized, or edge-driven, convection (e.g., Kim & So, 2020; King & Anderson, 1998) across heterogeneous LAB structure has also been recognized as an eroding force beneath the western Wyoming Craton (Dave & Li, 2016), and lithospheric edges are known to be inherently weak zones where upper mantle seismicity is most likely to nucleate (Jackson et al., 2021). Edge-driven convection has also been proposed as an important eroding force at the edges of cratonic lithosphere elsewhere in the western U.S. (e.g., Colorado Plateau in eastern Utah, van Wijk et al., 2010). Inherited shear zones from previous deformational episodes (e.g., Laramide basement thrusting) may provide additional weaknesses for strain localization (Fagereng et al., 2024; Prieto et al., 2017; Z. Zhu et al., 2021). Consistency with the regional crustal stress field supports mantle seismogenesis by the same regional forces suspected to be driving intraplate seismicity in the crust (Cao & Liu, 2024). This consistency further supports the link between intraplate seismicity and mantle forces driven by and interacting with complex lithospheric structure, as recognized in other regions experiencing intraplate deformation such as northern Europe (Bott et al., 2024).

Conflict of Interest

The authors declare no conflicts of interest relevant to this study.

Data Availability Statement

USGS ComCat is available from U.S. Geological Survey (2017). We downloaded waveform data from the Data Management Center (DMC) of the EarthScope Consortium (EarthScope, 2025) using seismic networks with codes: IM (Various Institutions, 1965), IW (Albuquerque Seismological Laboratory/USGS, 2003), MB (Montana Bureau of Mines and Geology/Montana Tech, 1982), TA (IRIS Transportable Array, 2003), US (Albuquerque Seismological Laboratory/USGS, 1990), UU (University of Utah, 1962), WY (University of Utah, 1983), and XV

(Sheehan et al., 2009). Herrmann (2025) and Klein (2019) detail instructions for downloading the latest versions of ELOCATE and HYPOINVERSE software, respectively.

Acknowledgments
We thank the many authors who shared their models of crustal thickness and other geophysical properties in the western U.S. Alysha Armstrong and Tessa Czech contributed to initial discussions as part of a graduate seminar class. Vera Schulte-Pelkum, Ben Baker, and Walter D. Mooney provided important comments on this work. We thank Seth Carpenter and an anonymous reviewer for detailed, cogent reviews. Seismic monitoring of Utah and southwestern Wyoming at the University of Utah is supported by the State of Utah and the U.S. Geological Survey (G20AC00036) under the Advanced National Seismic System. Seismic monitoring of the Yellowstone region at the University of Utah is supported by the volcano hazards programs of the U.S. Geological Survey (G21AC10068). Keith D. Koper acknowledges sabbatical support from the University of Utah. The seismic imaging work of Fan-Chi Lin is supported by the National Science Foundation (EAR1753362).

References

Albuquerque Seismological Laboratory (ASL)/USGS. (1990). United States National Seismic Network (USNSN) [Dataset]. *International Federation of Digital Seismograph Networks*. https://doi.org/10.7914/SN/US

Albuquerque Seismological Laboratory (ASL)/USGS. (2003). Intermountain West seismic network (Wyoming network) [Dataset]. *International Federation of Digital Seismograph Networks*. https://doi.org/10.7914/SN/IW

Becker, T. W., Lowry, A. R., Faccenna, C., Schmandt, B., Borsa, A., & Yu, C. (2015). Western US intermountain seismicity caused by changes in upper mantle flow. *Nature*, *524*(7566), 458–461. https://doi.org/10.1038/nature14867

Bedrosian, P. A., & Frost, C. D. (2023). Geophysical extent of the Wyoming Province, western USA: Insights into ancient subduction and craton stability. *GSA Bulletin*, *135*(3–4), 745–752. https://doi.org/10.1130/B36417.1

Bezada, M., Zhu, Z., Byrnes, J., & Ford, H. (2024). *Internal structure of the Wyoming craton lithosphere from geophysical imaging and its relationship to surface deformation*. American Geophysical Union Annual Meeting 2024 Abstracts. Retrieved from https://agu.confex.com/agu/agu24/meetingapp.cgi/Session/241116

Blackwell, D., Richards, M., Frone, Z., Batir, J., Ruzo, A., Dingwall, R., & Williams, M. (2011). Temperature-at-depth maps for the coterminous U. S. and geothermal resource estimates. *GRC Transactions*, *35*, 1545–1550. Retrieved from https://www.osti.gov/biblio/1137036

Bott, J., Scheck-Wenderoth, M., Kumar, A., Cacace, M., Noe, S., & Faleide, J. I. (2024). Density and strength variations in the mantle lithosphere affect the distribution of intraplate earthquakes. *Nature Communications Earth and Environment*, *5*(1), 243. https://doi.org/10.1038/s43247-024-01417-4

Buehler, J. S., & Shearer, P. M. (2017). Uppermost mantle seismic velocity structure beneath USArray. *Journal of Geophysical Research: Solid Earth*, *122*(1), 436–448. https://doi.org/10.1002/2016JB013265

Burgmann, R., & Dresen, G. (2008). Rheology of the lower crust and upper mantle: Evidence from rock mechanics, geodesy, and field observations. *Annual Review of Earth and Planetary Sciences*, *36*(1), 531–567. https://doi.org/10.1146/annurev.earth.36.031207.124326

Cao, Z., & Liu, L. (2024). Western US intraplate deformation controlled by the complex lithospheric structure. *Nature Communications*, *15*(1), 3917. https://doi.org/10.1038/s41467-024-48223-2

Castellanos, J. C., Humphreys, E., & Clayton, R. W. (2022). Evidence of mantle-based deformation across the western United States. *Geophysical Research Letters*, *49*(4), e2021GL094854. https://doi.org/10.1029/2021GL094854

Chen, W.-P., & Molnar, P. (1983). Focal depths of intracontinental and intraplate earthquakes and their implications for the thermal and mechanical properties of the lithosphere. *Journal of Geophysical Research*, *88*(B5), 4183–4214. https://doi.org/10.1029/JB088iB05p04183

Chen, W.-P., & Yang, Z. (2004). Earthquakes beneath the Himalayas and Tibet: Evidence for strong lithospheric mantle. *Science*, *304*(5679), 1949–1952. https://doi.org/10.1126/science.1097324

Chen, W.-P., Yu, C.-Q., Tseng, T.-L., Yang, Z., Wang, C.-Y., Ning, J., & Leonard, T. (2013). Moho, seismogenesis, and rheology of the lithosphere. *Tectonophysics*, *609*, 491–503. https://doi.org/10.1016/j.tecto.2012.12.019

Craig, T. J., & Heyburn, R. (2015). An enigmatic earthquake in the continental mantle lithosphere of stable North America. *Earth and Planetary Science Letters*, *425*, 12–23. https://doi.org/10.1016/j.epsl.2015.05.048

Dave, R., & Li, A. (2016). Destruction of the Wyoming craton: Seismic evidence and geodynamic processes. *Geology*, *44*(11), 883–886. https://doi.org/10.1130/G38147.1

EarthScope. (2025). Data Management Center [Dataset]. NSF SAGE. Retrieved from https://ds.iris.edu/ds/nodes/dmc/

Ekström, G., Nettles, M., & Dziewonski, A. M. (2012). The global CMT project 2004–2010: Centroid-moment tensors for 13,017 earthquakes. *Physics of the Earth and Planetary Interiors*, *200–201*, 1–9. https://doi.org/10.1016/j.pepi.2012.04.002

Fagereng, Å., Diener, J. F. A., Tulley, C. J., & Manda, B. (2024). Metamorphic inheritance, lower-crustal earthquakes, and continental rifting. *Geochemistry, Geophysics, Geosystems*, *25*(3), e2023GC011305. https://doi.org/10.1029/2023GC011305

Frohlich, C., Gan, W., & Herrmann, R. B. (2015). Two deep earthquakes in Wyoming. *Seismological Research Letters*, *86*(3), 810–818. https://doi.org/10.1785/0220140197

Golos, E. M., Fang, H., & van der Hilst, R. D. (2020). Variations in seismic wave speed and Vp/Vs ratio in North American lithosphere. *Journal of Geophysical Research: Solid Earth*, *125*(12), e2020JB020574. https://doi.org/10.1029/2020JB020574

Hasterok, D., & Chapman, D. S. (2011). Heat production and geotherms for the continental lithosphere. *Earth and Planetary Science Letters*, *307*(1–2), 59–70. https://doi.org/10.1016/j.epsl.2011.04.034

Herrmann, R. B. (2013). Computer programs in seismology: An evolving tool for instruction and research. *Seismological Research Letters*, *84*(6), 1081–1088. https://doi.org/10.1785/0220110096

Herrmann, R. B. (2025). Computer programs in seismology [Software]. *Stl*. Retrieved from https://rbherrmann.github.io/ComputerProgramsSeismology//index.html

Herrmann, R. B., Benz, H., & Ammon, C. J. (2011). Monitoring the earthquake source process in North America. *Bulletin of the Seismological Society of America*, *101*(6), 2609–2625. https://doi.org/10.1785/0120110095

Inbal, A., Ampuero, J. P., & Clayton, R. W. (2016). Localized seismic deformation in the upper mantle revealed by dense seismic arrays. *Science*, *354*(6308), 88–92. https://doi.org/10.1126/science.aaf1370

IRIS Transportable Array. (2003). USArray transportable array (Earthscope_TA) [Dataset]. *International Federation of Digital Seismograph Networks*. https://doi.org/10.7914/SN/TA

Jackson, J., McKenzie, D., & Priestley, K. (2021). Relations between earthquake distributions, geological history, tectonics and rheology on the continents. *Philosophical Transactions of the Royal Society A*, *378*(2193), 20190412. https://doi.org/10.1098/rsta.2019.0412

Kim, D.-H., & So, B.-S. (2020). Effects of rheology and mantle temperature structure on edge-driven convection: Implications for partial melting and dynamic topography. *Physics of the Earth and Planetary Interiors*, *303*, 106487. https://doi.org/10.1016/j.pepi.2020.106487

King, S. D., & Anderson, D. L. (1998). Edge-driven convection. *Earth and Planetary Science Letters*, *160*(3–4), 289–296. https://doi.org/10.1016/S0012-821X(98)00089-2

Klein, F. W. (2002). User's guide to HYPOINVERSE-2000, a Fortran program to solve for earthquake locations and magnitudes 4/2002 version. In *U.S. Geological Survey open file report* (Vol. 2002-171, pp. 1–122). U.S. Geological Survey. https://doi.org/10.3133/ofr02171

Klein, F. W. (2019). HYPOINVERSE earthquake location software release [Software]. *Stl*. Retrieved from https://www.usgs.gov/software/hypoinverse-earthquake-location

Lavayssière, A., Drooff, C., Ebinger, C., Gallacher, R., Illsley-Kemp, F., Oliva, S. J., & Keir, D. (2019). Depth extent and kinematics of faulting in the southern Tanganyika rift, Africa. *Tectonics*, *38*(3), 842–862. https://doi.org/10.1029/2018TC005379

Lebedev, S., Fullea, J., Xu, Y., & Banadio, R. (2024). Seismic thermography. *Bulletin of the Seismological Society of America*, *114*(3), 1227–1242. https://doi.org/10.1785/0120230245

Levander, A., & Miller, M. S. (2012). Evolutionary aspects of lithosphere discontinuity structure in the western U.S. *Geochemistry, Geophysics, Geosystems*, *13*(7), Q0AK07. https://doi.org/10.1029/2012GC004056

Lindenfeld, M., & Rümpker, G. (2011). Detection of mantle earthquakes beneath the East African rift. *Geophysical Journal International*, *186*, 1–5. https://doi.org/10.1111/j.1365-246X.2011.05048.x

Lindenfeld, M., Rümpker, G., Link, K., Koehn, D., & Batte, A. (2012). Fluid-triggered earthquake swarms in the Rwenzori region, East African rift—Evidence for rift initiation. *Tectonophysics*, *566-567*, 95–104. https://doi.org/10.1016/j.tecto.2012.07.010

Long, M. D., Levander, A., & Shearer, P. M. (2014). An introduction to the special issue of Earth and Planetary Science Letters on USArray science. *Earth and Planetary Science Letters*, *402*, 1–5. https://doi.org/10.1016/j.epsl.2014.06.016

Lucazeau, F. (2019). Analysis and mapping of an updated terrestrial heat flow data set. *Geochemistry, Geophysics, Geosystems*, *20*(8), 4001–4024. https://doi.org/10.1029/2019GC008389

Maggi, A., Jackson, J. A., Priestley, K., & Baker, C. (2000). A re-assessment of focal depth distributions in southern Iran, the Tien Shan and northern India: Do earthquakes really occur in the continental mantle? *Geophysical Journal International*, *143*(3), 629–661. https://doi.org/10.1046/j.1365-246X.2000.00254.x

Michailos, K., Carpenter, N. S., & Hetényi, G. (2021). Spatio-temporal evolution of intermediate-depth seismicity beneath the Himalayas: Implications for metamorphism and tectonics. *Frontiers in Earth Science*, *9*, 742700. https://doi.org/10.3389/feart.2021.742700

Molnar, P. (2020). The brittle-plastic transition, earthquakes, temperatures, and strain rates. *Journal of Geophysical Research: Solid Earth*, *125*(7), e2019JB019335. https://doi.org/10.1029/2019JB019335

Molnar, P., & Chen, W.-P. (1983). Focal depths and fault plane solutions of earthquakes under the Tibetan Plateau. *Journal of Geophysical Research*, *88*(B2), 1180–1196. https://doi.org/10.1029/JB088iB02p01180

Monsalve, G., Sheehan, A., Schulte-Pelkum, V., Rajaure, S., Pandey, M. R., & Wu, F. (2006). Seismicity and one-dimensional velocity structure of the Himalayan collision zone: Earthquakes in the crust and upper mantle. *Journal of Geophysical Research*, *111*(B10), B10301. https://doi.org/10.1029/2005JB004062

Montana Bureau of Mines and Geology/Montana Tech (MBMG, MT). (1982). Montana regional seismic network (MRSN) [Dataset]. *International Federation of Digital Seismograph Networks*. https://doi.org/10.7914/SN/MB

O'Rourke, C. T., Sheehan, A. F., Erslev, E. A., & Anderson, M. L. (2016). Small-magnitude earthquakes in north-central Wyoming recorded during the Bighorn Arch Seismic Experiment. *Bulletin of the Seismological Society of America*, *106*(1), 281–288. https://doi.org/10.1785/0120150114

Pankow, K. L., Stickney, M., Ben-Horin, J. Y., Litherland, M., Payne, S., Koper, K. D., et al. (2020). Regional seismic network monitoring in the eastern Intermountain West. *Seismological Research Letters*, *91*(2A), 631–646. https://doi.org/10.1785/0220190209

Priestley, K., Tak, H., Takei, Y., & Abercrombie, R. (2024). The thermal and anisotropic structure of the top 300 km of the mantle. *Earth and Planetary Science Letters*, *626*, 1118525. https://doi.org/10.1016/j.epsl.2023.118525

Prieto, G. A., Froment, B., Yu, C., Poli, P., & Abercrombie, R. (2017). Earthquake rupture below the brittle-ductile transition in continental lithospheric mantle. *Science Advances*, *3*, e1602642. https://doi.org/10.1126/sciadv.1602642

Pyle, M. L., Chen, T., Preston, L., Scalise, M., Zeiler, C., & Smith, K. D. (2023). How good is your location? Comparing and understanding the uncertainties in location for the 1993 rock valley sequence. *The Seismic Record*, *3*(4), 259–268. https://doi.org/10.1785/0320230025

Schmandt, B., Lin, F.-C., & Karlstrom, K. E. (2015). Distinct crystal isostasy trends east and west of the Rocky Mountain front. *Geophysical Research Letters*, *42*(23), 10290–10298. https://doi.org/10.1002/2015GL066593

Schulte-Pelkum, V., Monsalve, G., Sheehan, A. F., Shearer, P., Wu, F., & Rajaure, S. (2019). Mantle earthquakes in the Himalayan collision zone. *Geology*, *47*(9), 815–819. https://doi.org/10.1130/G46378.1

Schutt, D. L., Lowry, A. R., & Buehler, J. S. (2018). Moho temperature and mobility of lower crust in the western United States. *Geology*, *46*(3), 219–222. https://doi.org/10.1130/G39507.1

Sheehan, A., Miller, K., Anderson, M., Siddoway, C. S., & Erslev, E. (2009). Bighorn Arch Seismic Experiment [Dataset]. *International Federation of Digital Seismograph Networks*. https://doi.org/10.7914/SN/XV_2009

Shinevar, W. J., Golos, E. M., Jagoutz, L., Behn, M. D., & van der Hilst, R. D. (2023). Mantle thermochemical variations beneath continental United States through petrologic interpretation of seismic tomography. *Earth and Planetary Science Letters*, *602*, 117965. https://doi.org/10.1016/j.epsl.2022.117965

Skoumal, R. J., Hardebeck, J. L., & Shearer, P. M. (2024). SKHASH, version 1.0 [Software]. *Earthquake Science Center Gitlab*. Retrieved from https://code.usgs.gov/esc/SKHASH

Sloan, R. A., & Jackson, J. A. (2012). Upper-mantle earthquakes beneath the Arafura Sea and South Aru trough: Implications for continental rheology. *Journal of Geophysical Research*, *117*(B5), B05402. https://doi.org/10.1029/2011JB008992

Song, X., & Klemperer, S. L. (2024). Numerous Tibetan lower-crustal and upper mantle earthquakes, detected by *Sn*/*Lg* ratios, suggest crustal delamination or drip tectonics. *Earth and Planetary Science Letters*, *626*, 118555. https://doi.org/10.1016/j.epsl.2023.118555

Tesauro, M., Kaban, M. K., Mooney, W. D., & Cloetingh, S. A. P. L. (2014). Density, temperature, and composition of the North American lithosphere – New insights from a joint analysis of seismic, gravity, and mineral physics data: 2. Thermal and compositional model of the upper mantle. *Geochemistry, Geophysics, Geosystems*, *15*(12), 4808–4830. https://doi.org/10.1002/2014GC005484

Thielmann, M. (2018). Grain size assisted thermal runaway as a nucleation mechanism for continental mantle earthquakes: Impact of complex rheologies. *Tectonophysics*, *746*, 611–623. https://doi.org/10.1016/j.tecto.2017.08.038

University of Utah. (1962). University of Utah regional seismic network (Utah network) [Dataset]. *International Federation of Digital Seismograph Networks*. https://doi.org/10.7914/SN/UU

University of Utah. (1983). Yellowstone National Park seismograph network (Yellowstone) [Dataset]. *International Federation of Digital Seismograph Networks*. https://doi.org/10.7914/SN/WY

U.S. Geological Survey. (2017). Advanced National Seismic System (ANSS) comprehensive catalog of earthquake events and products: Various [Dataset]. *Earthquake Hazards Program*. https://doi.org/10.5066/F7MS3QZH

van Wijk, J. W., Baldridge, W. S., van Hunen, J., Goes, S., Aster, R., Coblentz, D. D., et al. (2010). Small-scale convection at the edge of the Colorado Plateau: Implications for topography, magmatism, and the evolution of Proterozoic lithosphere. *Geology*, *38*(7), 611–614. https://doi.org/10.1130/G31031.1

Various Institutions. (1965). International miscellaneous stations (IMS) [Dataset]. *International Federation of Digital Seismograph Networks*. https://doi.org/10.7914/vefq-vh75

Wang, S., & Klemperer, S. L. (2021). Love-wave normal modes discriminate between upper-mantle and crustal earthquakes: Simulation and demonstration in Tibet. *Earth and Planetary Science Letters*, *571*, 117089. https://doi.org/10.1016/j.epsl.2021.117089
Wiens, D. A., & McGuire, J. J. (1995). The 1994 Bolivia and Tonga events: Fundamentally different types of deep earthquakes? *Geophysical Research Letters*, *22*(16), 2245–2248. https://doi.org/10.1029/95GL01598
Wong, I. G., & Chapman, D. S. (1990). Deep intraplate earthquakes in the western United States and their relationship to lithospheric temperatures. *Bulletin of the Seismological Society of America*, *80*, 589–599. https://doi.org/10.1785/BSSA0800030589
Yang, Z., & Chen, W.-P. (2010). Earthquakes along the East African Rift system: A multiscale, system-wide perspective. *Journal of Geophysical Research*, *115*(B12), B12309. https://doi.org/10.1029/2009JB006779
Zandt, G., & Richins, W. D. (1979). An upper mantle earthquake beneath the middle Rocky Mountains in northeast Utah. *Earthquake Notes*, *50*, 69–70. https://doi.org/10.1130/MEM172-p541
Zeng, Q., Lin, F.-C., & Tsai, V. C. (2024). Spurious Rayleigh wave anisotropy near major structural boundaries: A numerical and theoretical investigation. *Geophysical Journal International*, *239*(2), 901–913. https://doi.org/10.1093/gji/ggae305
Zhan, Z. (2020). Mechanisms and implications of deep earthquakes. *Annual Review of Earth and Planetary Science*, *48*(1), 147–174. https://doi.org/10.1146/annurev-earth-053018-060314
Zhao, D., Liang, Z., Toyokuni, G., Hua, Y., & Xu, Y.-G. (2024). Cause of enigmatic earthquakes in central Wyoming. *Seismological Research Letters*, *95*(4), 2497–2505. https://doi.org/10.1785/0220230333
Zhu, L., & Helmberger, D. V. (1996). Intermediate depth earthquakes beneath the India-Tibet collision zone. *Geophysical Research Letters*, *23*(5), 435–438. https://doi.org/10.1029/96GL00385
Zhu, Z., Bezada, M. J., Byrnes, J. S., & Ford, H. A. (2021). Evidence for stress localization caused by lithospheric heterogeneity from seismic attenuation. *Geochemistry, Geophysics, Geosystems*, *22*(11), e2021GC009987. https://doi.org/10.1029/2021GC009987

References From the Supporting Information

Bjarnason, I. T., & Pechmann, P. C. (1989). Contemporary tectonics of the Wasatch front region, Utah, from earthquake focal mechanisms. *Bulletin of the Seismological Society of America*, *79*, 731–755. https://doi.org/10.1785/BSSA0790030731
Brumbaugh, D. A. (2001). *The 1994 Draney Peak, Idaho, earthquake sequence: Focal mechanisms and stress field inversion*. Thesis. University of Utah.
Buehler, J. S., & Shearer, P. M. (2010). Pn tomography of the western United States using the USArray. *Journal of Geophysical Research*, *115*(B9), B09315. https://doi.org/10.1029/2009JB006874
Buehler, J. S., & Shearer, P. M. (2014). Anisotropy and Vp/Vs in the uppermost mantle beneath the western United States from joint analysis of Pn and Sn phases. *Journal of Geophysical Research: Solid Earth*, *119*(2), 1200–1219. https://doi.org/10.1002/2013JB010559
Chulick, G. S., & Mooney, W. D. (2002). Seismic structure of the crust and uppermost mantle of North America and adjacent oceanic basins: A synthesis. *Bulletin of the Seismological Society of America*, *92*(6), 2478–2492. https://doi.org/10.1785/0120010188
Gilbert, H. (2012). Crustal structure and signatures of recent tectonism as influenced by ancient terranes in the western United States. *Geosphere*, *8*(1), 141–157. https://doi.org/10.1130/GES00720.1
Gomberg, J. S., Shedlock, K. M., & Roecker, S. W. (1990). The effect of S-wave arrival times on the accuracy of hypocenter estimation. *Bulletin of the Seismological Society of America*, *80*(6A), 1605–1628. https://doi.org/10.1785/BSSA08006A1605
Kennett, B. L. N., Engdahl, E. R., & Buland, R. (1995). Constraints on seismic velocities in the earth from travel times. *Geophysical Journal International*, *122*(1), 108–124. https://doi.org/10.1111/j.1365-246X.1995.tb03540.x
Laske, G., Masters, G., Ma, Z., & Pasyanos, M. (2013). Update on CRUST1.0 - A 1-degree global model of Earth's crust. *Geophysical Research Abstracts*, *15*. Retrieved from https://meetingorganizer.copernicus.org/EGU2012/EGU2012-3743-1.pdf
Lowry, T., & Perez-Gussinye, M. (2011). The role of crustal quartz in controlling Cordilleran deformation. *Nature*, *471*(7338), 353–357. https://doi.org/10.1038/nature09912
Ma, X., & Lowry, A. R. (2017). USArray imaging of continental crust in the conterminous United States. *Tectonics*, *36*(12), 2882–2901. https://doi.org/10.1002/2017TC004540
Pechmann, J. C., Brumbaugh, D. A., Nava, S. J., Skelton, T. G., Fivas, G. P., Arabasz, W. J., & Jackson, S. M. (1997). The 1994 Draney Peak, ID, earthquake and its aftershocks. *EOS Trans. AGU*, *78*, F480.
Pechmann, P. C., Arabasz, W. J., Pankow, K. L., & Jensen, M. E. (2002). Appendix B: Seismic velocity model for the Trail mountain area. In *Ground motion recording and analysis of mining induced seismicity in the Trail mountain area, Emery County, Utah, technical report* (pp. B1–B9). State of Utah School and Trust Lands Administration.
Richins, W. D., Arabasz, W. J., Hathaway, G. M., Oemich, P. J., Sells, L. L., & Zandt, G. (1981). *Earthquake data for the Utah region, July 1, 1978 to December 31, 1980* (p. 127). University of Utah Seismograph Stations Special Publication. Retrieved from https://quake.utah.edu/earthquake-information-products/earthquake-catalogs/catalog-details
Shehata, M. A., & Mizunaga, H. (2022). Moho depth and tectonic implications of the western United States: Insights from gravity data interpretation. *Geoscience Letters*, *9*(1), 9–23. https://doi.org/10.1186/s40562-022-00233-y
Shen, W., & Ritzwoller, M. H. (2016). Crustal and uppermost mantle structure beneath the United States. *Journal of Geophysical Research: Solid Earth*, *121*(6), 4306–4342. https://doi.org/10.1002/2016JB012887
Tichelaar, B. W., & Ruff, L. J. (1989). How good are our best models? Jackknifing, bootstrapping, and earthquake depth. *EOS*, *70*(20), 593–606. https://doi.org/10.1029/89EO00156
Wadati, K. (1928). Shallow and deep earthquakes. *Geophysical Magazine*, *1*, 161–202.
Zeiler, C. P., Stickney, M. C., & Speece, M. A. (2005). Revised velocity structure of western Montana. *Bulletin of the Seismological Society of America*, *95*(2), 759–762. https://doi.org/10.1785/0120040088
Zhang, H. L., Ravat, D., & Lowry, A. R. (2020). Crustal composition and Moho variations of the Central and Eastern United States: Improving resolution and geologic interpretation of Earthscope USArray seismic images using gravity. *Journal of Geophysical Research: Solid Earth*, *125*(3), e2019JB018537. https://doi.org/10.1029/2019JB018537